2017 IEEE International Conference on Advanced Intelligent Mechatronics (AIM)
Sheraton Arabella Park Hotel, Munich, Germany, July 3-7, 2017

Mechanical Stiffness Control of a Three DOF Wrist Joint that Mimics Musculo-skeletal System

Koichi Koganezawa

Abstract— **This paper shows a prosthetic wrist joint that has 3 rotary axes controlled in antagonistic actuation similar to a human musculo-skeletal system. Some dexterous actions of human arm toward external entities are much attributed to adjustability of its joint stiffness. The joint stiffness of human articulations or of those of any other vertebrate animals is adjustable due to an antagonistic structure of their musculoskeletal system and non-linear elasticity of individual muscle. In our previous studies we have developed a mechanical system that mimics the human musculoskeletal system, in which muscle-like actuators: ANLES (actuator with non-elasticity system) was developed and deployed in antagonistic configuration to control rotation angles and rotary stiffness of a multi-DOF robotic joint. This paper shows a subsequent development of the 3 DOF wrist joint. Main points of refinement are as follows. First is a downsizing to serve it as a forearm prosthesis having an active wrist joint, second is an extension of stiffness adjustable range especially that of inner/outer rotation.**

I. Introduction

For disabled persons who lost their arm by occupational or traffic accidents, forearm prosthetic hand is essential for improving their QOL. However, in the conventional developments of forearm prosthesis [1] has focused only on the hand with movable fingers with less concerning about a wrist joint acting like Fig1. When we look at hand tasks in our life, it is easily recognized that the wrist joint is indispensable for the hand achieving some dexterous motions that has an interaction with some external entities (opening a door, writing or drawing with pen, throwing a ball, etc.) . Human arm achieves some dexterous works due to its sophisticated control of stiffness of joint that means how much the joint rotates in response to an externally loaded torque , which is explicitly defined as a derivative of torque τ with respect to the resultant rotation angle θ ((1)).

$$S = \partial\tau / \partial\theta \quad (1)$$

In a human musculo-skeletal system (Fig. 2), the joint stiffness changes with a pair of muscles allocated to provides a counteractive action to the joint (Fig. 3), in which it is prerequisite that individual muscle has a non-linear elasticity. Let us assume a joint be in an equilibrium state in terms of torque that a pair of muscles apply to the joint counteractively. As shown in Fig. 3 non-linear elasticity of a pair of muscles requires a large amount of Δτ to yield the same Δθ when they are in a high stretching state comparing to that in a low stretching state. Therefore human articulations adjusts the stiffness in a mechanical and structural basis. Our research purpose is to construct a robotic joint that has a similar

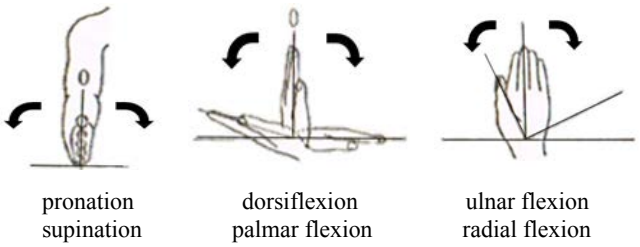

Fig. 1 Three rotations of wrist [2]

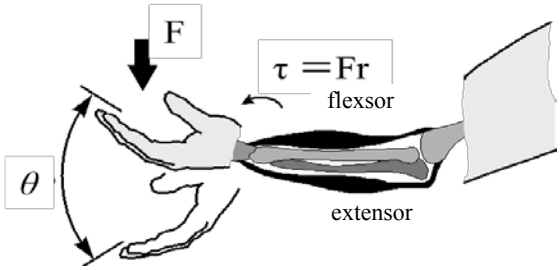

Fig. 2 A human musculo-skeletal system [3]

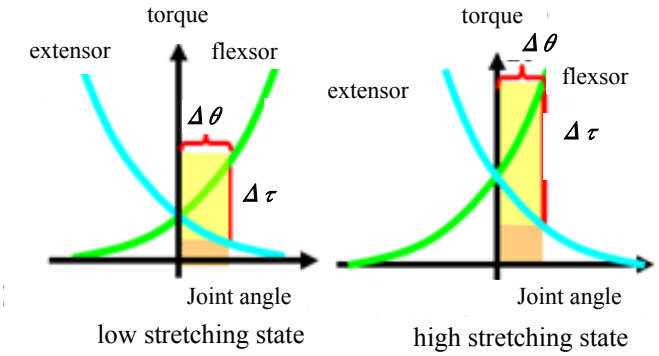

Fig. 3 Torque balancing state of two counteractive muscles

structure to the human musculo-skeletal system to change stiffness efficiently. This paper features a wrist joint that not only rotates about three rotation axes but also regulates the rotation stiffness using a mechanical module called *Actuator with Non-Linear Elasticity System* (ANLES).

II. ANLES

ANLES is a mechanical module that works like a human muscle, of which appearance and typical sizes are shown in Fig. 4(a) [4-5]. It consists of a long lead ball screw (rod

* Koichi Koganezawa is with the Dept. of Mechanical Engineering, Tokai University, 4-1-1 Kitakaname Hiratsuka City, Kanagawa,259-1292 ,Japan kogane@keyaki.cc.u-tokai.ac.jp

(a) Assembled view of ANLES

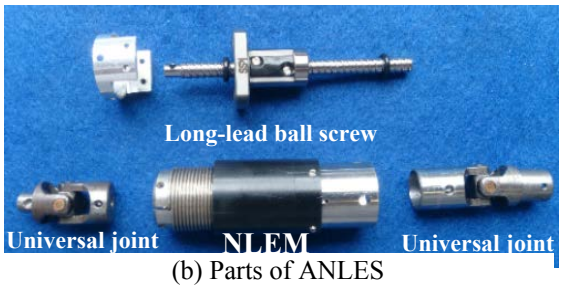

(b) Parts of ANLES

(c) Parts of NLEM

Fig. 4 ANLES; out view and the parts

diameter: 6 mm, screw lead: 6 mm) and Non-Linear Elasticity Module (NLME) (Fig. 4(b)) that consists of a torsion spring and a guide shaft (Fig. 4(c)). Rotating ANLES by a motor induces torsion spring winding and wrapping around the guide shaft of which taper form of the diameter yields a strictly designed non-linear elasticity of the spring.

Torque T_g yielded by the torsion spring is simply determined by the torsion angle ϕ with,

$$T_g = (EI/l_r)\phi \qquad (2)$$

where, E is the modulus of longitudinal elasticity, I is the second moment of area of the torsion spring and l_r is an expansion length of the spring portion that does not yet wrap the guide shaft. We can obtain the relation between the torsion angle $\phi(x)$ and the torque $T_g(x)$ as functions of the axial position parameter x, which can be combined to produce a function $T_g(\phi)$. Therefore, we can design the function $T_g(\phi)$ through designing $r(x)$: the function of the radius at an axial position x (Fig. 5).

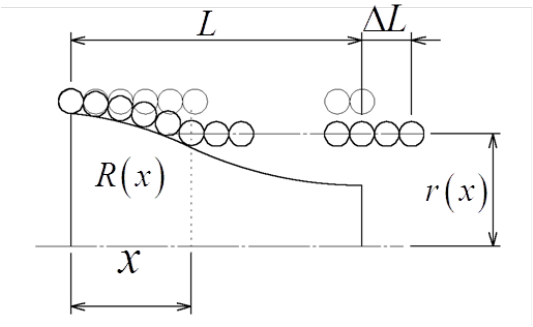

Fig. 5 Model of Guide-shaft

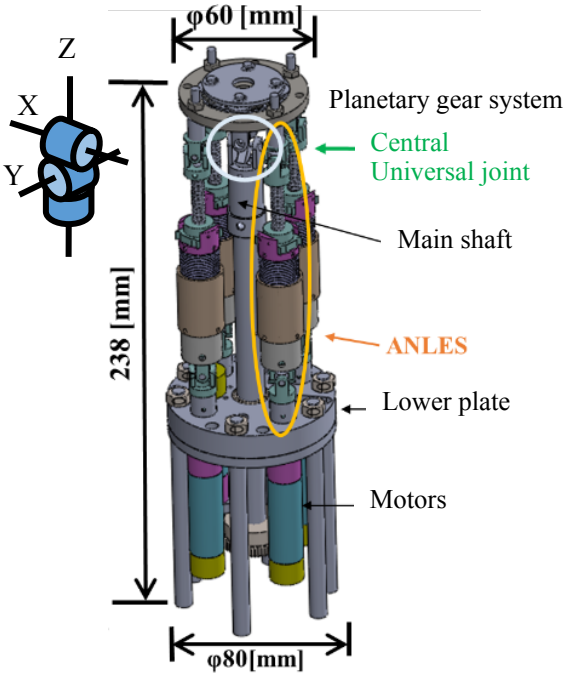

Fig. 6 Assembly of the test machine

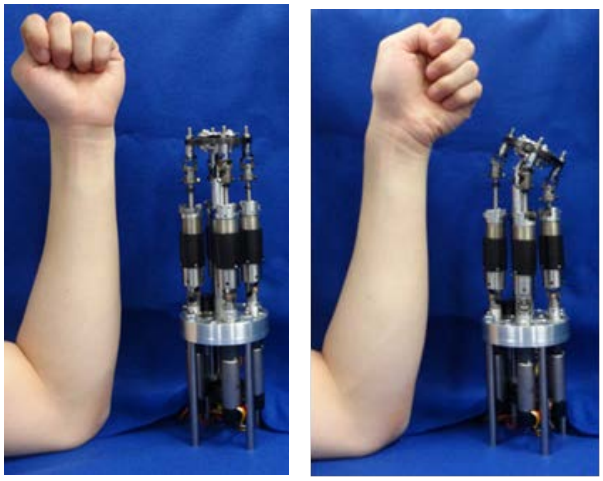

Fig. 7 Size comparison with human forearm

III. 3 DOF Wrist Joint

We develop a robotic forearm with wrist joint that employs 4 ANLES as artificial muscles and additional one motor to rotate the main shaft (Fig. 6). This forearm is almost the same size as human arm (see Fig.7) [7].

Rotation of a pair of ANLES in opposite rotary direction induces axial sliding of the ball-screw rod in the opposite linear direction, which makes the wrist joint rotate. In contrast, rotation of the pair of ANLES in a common direction makes the torsion springs wind around the guide shafts, which

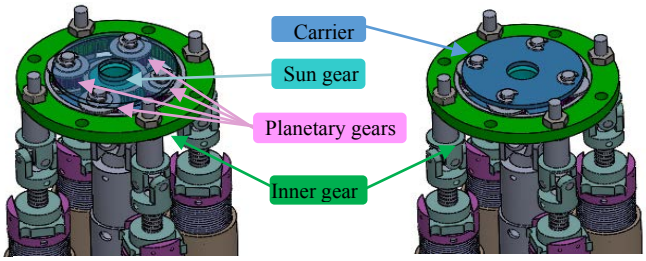

Fig. 8 Planetary gear system as the upper plate

induces the joint stiffness changes. Hence the wrist joint is capable of regulating stiffness about X,Y axes as well as controlling their rotation angles. The main shaft is directly rotated by the fifth motor to make the wrist joint rotate about Z axis. The stiffness about Z axis is also changeable via the planetary gear system constituting an upper plate (Fig. 6) , in which four ANLES are connected to the inner gear via individual universal joint (see Fig. 8). An end-effector (hand) is connected to the carrier. When some external torque or force is applied to the end-effector, which provides some torque to the carrier, it induces a rotation of the inner gear with accompanying the four ANLES tilting around the main shaft, which induces the torsion springs of four ANLES twisting although the solar gear that is connected to the main shaft stands still. Therefore the stiffness of the Z axis is determined by initial torsion angle of the torsion springs of four ANLES, which means the stiffness of the Z-axis is not independent to those of the X and Y axes; it is determined concomitantly with those about X and Y axes.

Rotation angles of X and Y axes are measured by the individual eddy current gap sensors embedded at the upper and lower portions of the central universal joint (Fig.9); the sensors measures a gap length between the sensor and the surface of the cam-shape dice of the central universal joint. The reason why this joint angle sensors are employed is that there is no space to put rotary angle sensors such as encoder or potentiometer outside the central universal joint, where four ANLES are deployed and move over (see Fig.10).

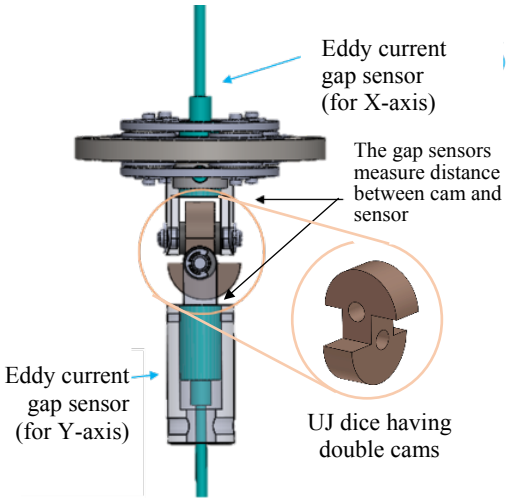

Fig. 9 Two axes angle sensor system

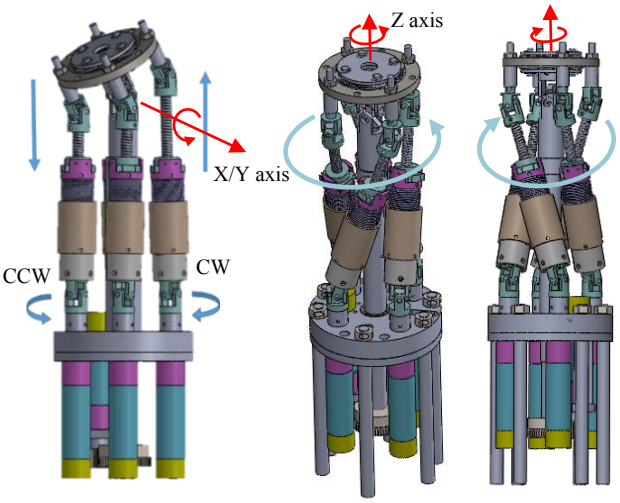

(a) X,Y axes rotations (b) Z axis rotation

Fig.10 Three axes rotations

IV. Experiment for Measuring Stiffness

From Eq.(1), measuring the torque $\Delta\tau$ that produces the wrist joint rotation by $\Delta\theta$, provides the joint stiffness that will be a function of twisting angle of the torsion spring of four ANLES. The experimental procedures are as follows:

1) The angles of X, Y and Z axes are set 0 degree.
2) The torsion coil springs of four ANLES are twisted by the same angle by PID control of the individual motors.
3) Torque are given about X, Y or Z axis in a way that some horizontal tension ΔF [N] is gradually applied to the rod connected to the carrier of the planetary gear until the axis rotates a predetermined small angle $\Delta\theta$ degrees.
4) The stiffness is estimated by $s = \Delta F \times r / \Delta\theta$ [Nm/deg] with a moment arm r. Here, 5 degrees is used as $\Delta\theta$.

Fig.11 shows the experimental results of the stiffness variation about X, Y and Z axes. The error bars indicates variations of the experimental data of 5 trials. As shown the stiffness about X, Y and Z axes of the wrist joint concomitantly increase monotonically as twisting angle of four ANLES increases. The stiffness about X and Y axes are almost the same, but that about Z axis takes a fairly small value (about one third) comparing to those about X and Y axes, the reason of which is as follows. Rotation about X or Y axes induces a direct push or pull motion of the ball-screw rods (see Fig. 10), whereas, Z axis rotation (see also Fig. 10) makes all ANLES incline around the main shaft. This

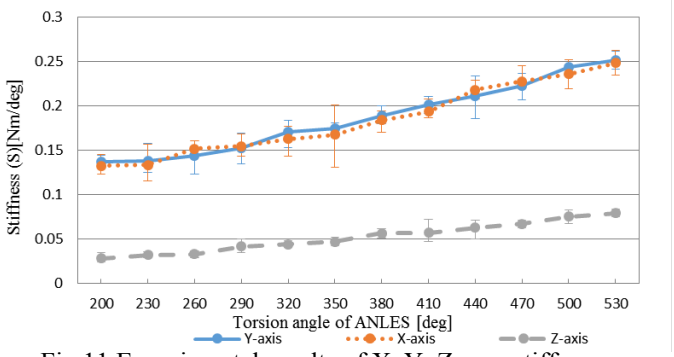

Fig.11 Experimental results of X, Y, Z axes stiffness

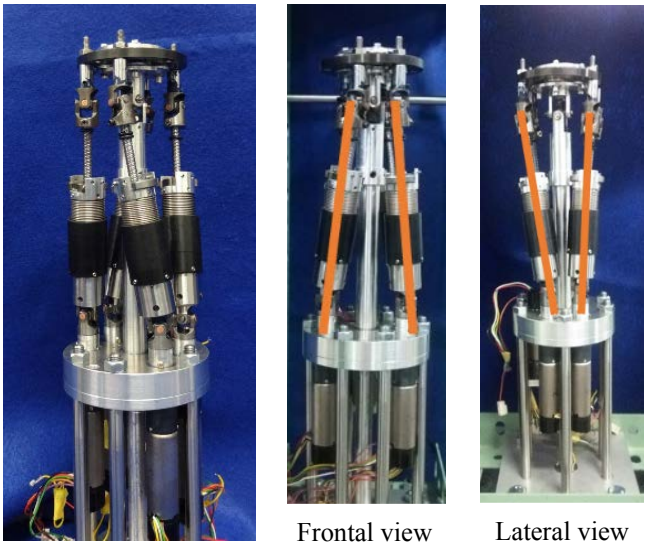

Frontal view Lateral view

Fig. 12 Improvement of wrist joint: ANLES are inclined

inclination also accompanies a push or pull motion of the ball-screw rods, but the amount of which is fairly small, because the derivative of push/pull motion of the ball-screw rods with respect to Z axis rotation angle start from zero in the layout of connection between ANLES and the planetary gear system shown in Fig. 8.

V. Improvement of the Wrist Joint

A. Augmentation of stiffness about Z-axis

In order to augment the stiffness about Z axis, the layout of four ANLES is altered as shown in Fig. 12. ANLES are connected to the lower plate and the planetary gear system with some inclined angle. This layout is expected to augment the stiffness especially about Z-axis because the derivative of push/pull length of ball screw rods with respect to Z-axis rotation angle has non-zero value.

Fig. 13 shows is the stiffness of X,Y,Z-axes in the inclined layout. The error bars indicates variations of the experimental data of 5 trials. By comparing with Fig. 11 we see almost twice increase of Z-axis stiffness. We also observe a slight increase of stiffness about Y-axis due to the effect of the inclination of ANLES. It should be noted that the adjustable

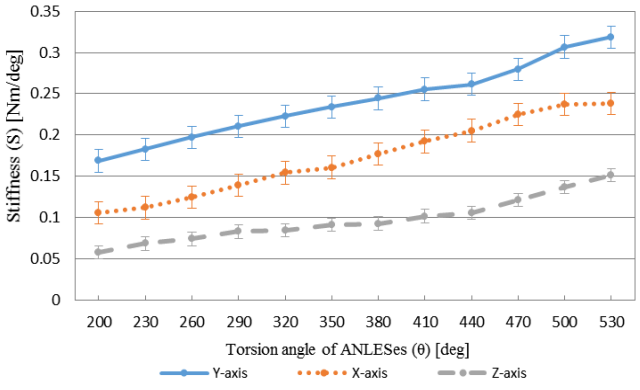

Fig. 13 X, Y, Z-axes stiffness in the inclined layout of ANLES

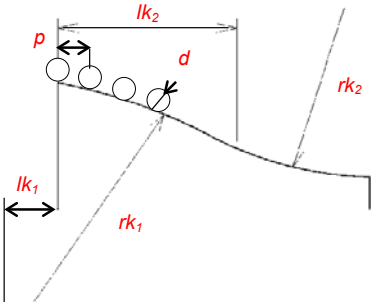

Fig.14 Design parameters of ANLES

range of the stiffness of all axes is extended by the inclined layout.

Table 1 Parameters of old and new guide shaft

		Old	*New*
Position of the center of the first curvature along axis [mm]	*lk1*	-8.8	-50
Changing position of curvatures [mm]	*lk2*	21.6	25
Radius of the first curvature [mm]	*rk1*	359	400
Radius of the second curvature [mm]	*rk2*	320	0
Diameter of the spring [mm]	*d*	0.8	1.2
Pitch of the spring [mm]	*p*	1.0	1.0
Winding number of the spring	*n*	24	24
Maximum radius of the guide shaft [mm]	*R0*	8	8
Minimum radius of the guide shaft [mm]	*R1*	7	4
The length of the guide shaft [mm]	*L*	24	24

B. New design of guide shaft and spring

Next we redesign the shape of the guide-shaft to expand the adjustable range of stiffness. According to the design parameters of the guide-shaft shown in Fig. 14, we find that their new values (Table 1) provides a nearly quadratic curve in the torque-torsion angle relation as shown in Fig. 15 (see the *Appendix 1*), which is expected to provide a nearly linear function in the stiffness-torsion angle relation because stiffness is fundamentally determined by the derivative of the torque with respect to the torsion angle, although it is affected with the layout of ANLES. Meanwhile, in the old guide shaft torque rapidly increases as the torsion angle takes 9 to 10 rad.

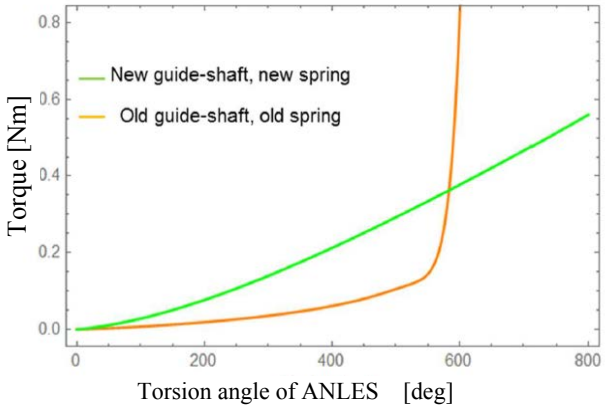

Fig. 15 Theoretical curve of the torque and the torsion angle of the spring

old new

Fig. 16 Appearance of the old and new guide-shafts

Fig. 16 shows the newly fabricated guide-shaft and the old guide-shaft. It should be noted that the wire-diameter of the spring is altered from 0.8 [mm] to 1.2[mm], which provides almost twice value of the yielding torque.

VI. Stiffness Improvement

With some improvements of the wrist joint denoted above, stiffness about the three axes are measured again. The measurement procedures are the same as those of descrived in IV. The error bars indicates variations of the experimental data of 5 trials. It is apparent that substantial improvenent in terms of the stiffness adjustability was achieved. Especially the stiffness of the Z-axis was prominently improved in its value. Its maximum value is beyond 1 [Nm/deg], which allows only 2 [deg] when loading 5 [kg] weight tangentially to the upper plate. The experimental results fairly differs from the theoretical curve. It is mainly due to the friction yieling inside the ball-screw nut. However the error bars are so small that the theoretical consideration taking into consideration of friction model is necessary.

VII. Conclusions

We have developed the three DOF wrist joint that mimics a human musculo-skeletal system. ANLES (Actuator with Non-Linear Elastic System), our developed actuator module, has a role of voluntary muscles. The beneficial points of ANLES are as follows.

(a) Non-linear elasticity that is a crucial property as a muscle can be strictly designed.

(b) It is controlled by a normal electric motor, no need for air-hoses and compressor that are necessary for pneumatic artificial muscle[6].

This paper described some improvements of the wrist joints of which main points are as follows.

(i) The ANLES are allocated in a little slanted posture (Fig.12), which augments the stiffness of the Z-axis. Probably human muscles are allocated in a similar manner.

(ii) The guide-shaft of which shape determines the non-linear elasticity is improved to provide high stiffness and wide range of stiffness adjustment.

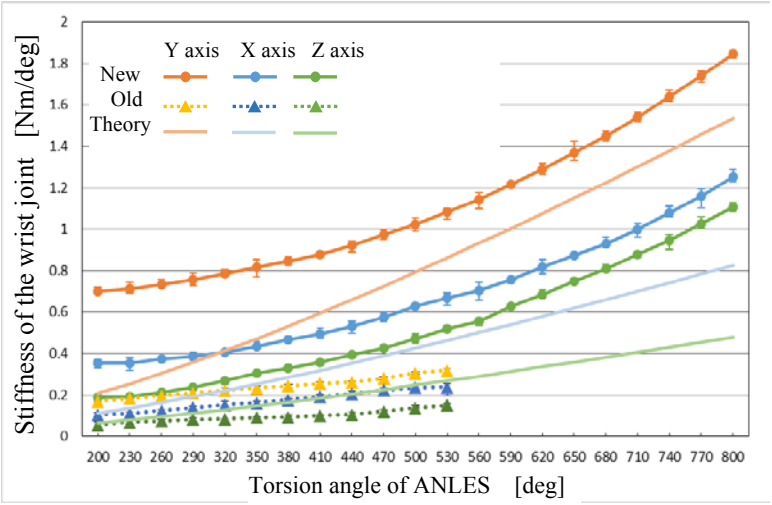

Fig. 17 Comparison of the stiffness of the three axes: new model, old model and theoretical curve

(iii) The weight is reduced from 1.53 [kg] to 1.07 [kg], which is lighter than 1.2 [kg]; the weight of normal adult male forearm[7]. It gives us a prospect to use it as a forearm prosthesis.

REFERENCES

[1] Harada Electronics Industry Ltd. , SH-2 , http://www.h-e-i.co.jp/Products/e_m_g/ph_sh_2.html

[2] Nakamura Ryuuiti, Saitou hirosi, Basic kinesiology, 2nd ed. , pp45, 1984

[3] Donald A. Neumann, Kinesiology muscle, pp259, 2005.

[4] K. Koganezawa, H. Yamashita, Stiffness Control of Multi-DOF Joint, Proc. Of 2009 IEEE/RSJ Int. Conf. on Intelligent Robots and Systems (IROS), St. Louis, Missouri, 2009.

[5] K. Koganezawa, G. Takami, M. Watanabe, Antagonistic Control of Multi-DOF Joint, 2012 IEEE/RSJ International Conference on Intelligent Robots and Systems(IROS), pp.2895-2900, 2012.

[6]Taro Nakamura, Daisuke Tanaka, Hiroyuki Maeda, "Joint Stiffness and Position Control of an Artificial Muscle Manipulator for Instantaneous Loads Using a Mechanical Equilibrium Model", Advanced Robotics, Vol.25, No.3, pp. 387-406, (2011)

[7] National Institute of Technology and Evaluation, Human characteristics database, http://www.tech.nite.go.jp/human/jp /contents/cindex/database.html

Appendix 1

Let us assume that the spring is twisted and wraps on the guide shaft from the left edge to the position x along the guide shaft axis (see Fig.5). The expansion length of the spring wrapping the guide shaft $\ell_a(x)$ is calculated as,

$$\ell_a(x) = \int_0^x \sqrt{1 + \left(2\pi(r(x) + d/2)/p(x)\right)^2}\, dx \qquad \text{(A-1)}$$

where, $r(x)$ is a radius of the spring at x with $r(0)=R$, which is designed as a differentiable function about x. $p(x)$ is the pitch of the spring that is getting to shorten as the twisting advances. Therefore it is a function of x. The coiling number $n(x)$ in the part of not yet wrapped on the guide shaft is,

$$n(x) = \left(\ell_T - \ell_a(x)\right) / \sqrt{\left(2\pi(r(x) + \mathrm{d}/2)\right)^2 + p(x)^2}$$

where, ℓ_T is a total expansion length of the spring. Hence the pitch when the spring wraps by position x is calculated as,

$$p(x) = \frac{L-x}{n(x)} = \frac{(L-x)\sqrt{\left(2\pi(r(x)+\mathrm{d}/2)\right)^2 + p(x)^2}}{\ell_T - \ell_a(x)} \quad \text{(A-2)}$$

Differentiating (A-1) with respect to x, we have,

$$d\ell_a(x)/dx = \sqrt{1+\left(2\pi(r(x)+d/2)/p(x)\right)^2}$$

Substituting $p(x)$ that is obtained from (A-2)

$$d\ell_a(x)/dx = \left(\ell_T - \ell_a(x)\right)/(L-x) \quad \text{(A-3)}$$

Solving (A-3) with an initial value; $\ell_a(0) = 0$, we have

$$\ell_a(x) = (l_T/L)x \quad \text{(A-4)}$$

Surprisingly, ℓ_a is linear with respect to x and does not depend on $r(x)$. Torsion angle of the spring $\phi(x)$ when it wraps on the guide shaft by x is found in the following relation,

$$2\pi(\ell_T - \ell_a(x))/\sqrt{\left(2\pi(R+d/2)\right)^2 + p(0)^2} + \phi(x) =$$
$$2\pi(\ell_T - \ell_a(x))/\sqrt{\left(2\pi(r(x)+d/2)\right)^2 + p(x)^2}$$

Substituting (A-2) and (A-4) we have $\phi(x)$ with simple mathematical operation,

$$\phi(x) = \left(1-\frac{x}{L}\right)\sqrt{\ell_T^2 - L^2}\left(\frac{1}{r(x)+d/2} - \frac{1}{R+d/2}\right) \quad \text{(A-5)}$$

Additional torque necessary to twist $d\phi(x)$ from a current torsion angle $\phi(x)$ is inversely proportional to the expansion length of the spring $\ell_T - \ell_a(x)$ as follows;

$$dT_a(x) = \frac{EI}{\ell_T - \ell_a(x)}d\phi(x) = \frac{EI}{\ell_T(1-x/L)}d\phi(x)$$

where, E is the modulus of longitudinal elasticity and I is the second moment of area of the torsion spring wire. Differentiating $\phi(x)$ with respect to x and substituting above, we have,

$$dT_a(x) = -EI\sqrt{\ell_T^2 - L^2}/\ell_T \times$$
$$\left(\frac{dx}{L-x}\left(\frac{1}{r(x)+d/2} - \frac{1}{R+d/2}\right) + \frac{dr(x)}{\left(r(x)+d/2\right)^2}\right) \quad \text{(A-6)}$$

Integrating (A-6) with $T_a(0) = 0$ and combined with the result of (A-5) we have $T_a(\phi)$ without using an intermediate variable x.

Appendix 2

Connecting points of ANLES at the lower plate A_L, B_L, C_L and D_L are defined by the constant vectors in Fig.18, a_L, b_L, c_L and d_L. The origin of universal joint O_{UL} is located at, $O_{UL} = (0 \quad 0 \quad l_L)^T$ The origin of the upper is calculated by,

$$O_{UP} = O_{UL}R_XR_YR_Z(0\ 0\ l_U)^T \quad \text{(A-6)}$$

where R_X, R_Y, R_Z are rotation matrices defined by,

$$R_X = \begin{bmatrix}1 & 0 & 0\\ 0 & c\theta_x & -s\theta_x\\ 0 & s\theta_x & c\theta_x\end{bmatrix},\ R_Y = \begin{bmatrix}c\theta_Y & 0 & s\theta_Y\\ 0 & 1 & 0\\ -s\theta_Y & 0 & c\theta_Y\end{bmatrix},\ R_Z = \begin{bmatrix}c\theta_Z & -s\theta_z & 0\\ s\theta_z & c\theta_z & 0\\ 0 & 0 & 1\end{bmatrix}$$

The location of the connecting point of ANLES at the upper plate, A_U, B_U, C_U and D_U from the origin of the upper plate O_{UP} are designated in the upper plate coordinate system, $a_U^{(U)}, b_U^{(U)}, c_U^{(U)}$ and $d_U^{(U)}$, where the superscript (U) designates a coordinate system. The position vectors of, A_U, B_U, C_U and D_U from the O_{LP} located at the lower plate are calculated by

$$(*)_U = O_{UP} + R_XR_YR_Z(*)_U^{(U)},\ ((*) = \mathrm{a, b, c, d}) \quad \text{(A-7)}$$

Vectors of the ANLES from the connecting point of the upper plate to those of the lower plate are obtained from,

$$n_{(*)} = (*)a_U - (*)_L,\ ((*) = a, b, c, d) \quad \text{(A-8)}$$

Infinitesimal variations of n_a, n_b, n_c and n_d cause by infinitesimal rotations of θ_x, θ_Y, θ_Z are,

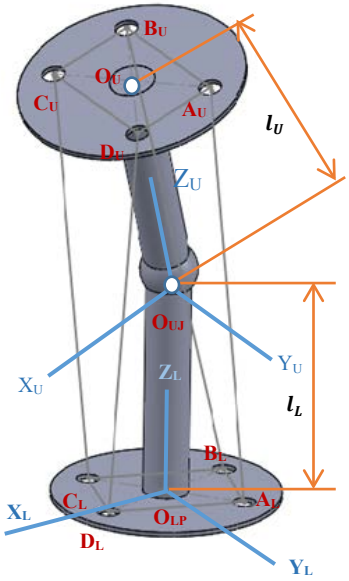

Fig.18 Model of the three D.O.F wrist joint controlled by 4 ANLES

$$\Delta n_i = \frac{\partial n_i}{\partial\theta_x}\Delta\theta_x + \frac{\partial n_i}{\partial\theta_Y}\Delta\theta_Y + \frac{\partial n_i}{\partial\theta_Z}\Delta\theta_Z,\ (i = a, b, c, d) \quad \text{(A-9)}$$

The variation of the length of the ANLES induces to twist the torsion spring of the ANLES,

$$\Delta\phi_i = \frac{2\pi}{L}(|n_i + \Delta n_i| - |n_i|)\ \ (\mathrm{i = a, b, c, d}) \quad \text{(A-10)}$$

where, L is a pitch of the ball-screw rod. This variation of the twisting angle of the ANLES induces the torque variation that the ANLES generates,

$$\tau(\bar{\phi}_i + \Delta\phi_i) \cong \tau(\bar{\phi}_i) + \left.\frac{\partial\tau}{\partial\phi_i}\right|_{\phi_i=\bar{\phi}_i}\Delta\phi_i \quad \text{(A-11)}$$

where, $\bar{\phi}_i$ is a torsion angle of the ith ANLES that is initially assigned. $\tau(\phi_i)$ is a non-linear function of the torque with respect to the torsion angle ϕ_i, of which non-linearity is designed by the shape of the guide-shaft of the ANLES (Appendix 1). The long-lead ball-screw transforms torque to force as follows,

$$F(\bar{\phi}_i + \Delta\phi_i) = \frac{2\pi}{L}\tau(\bar{\phi}_i + \Delta\phi_i) \quad \text{(A-12)}$$

This ith force is a magnitude of the force vector that has the ith unit vector $n_i/|n_i|$ (i=a, b, c, d)

$$F_i = \frac{n_i}{|n_i|}\mathrm{F}(\bar{\phi}_i + \Delta\phi_i) \quad (\mathrm{i = a, b, c, d}) \quad \text{(A-13)}$$

With the vectors from O_{UJ} (the origin of the universal joint) to A_U, B_U, C_U, D_U as,

$$r_{(*)} = R_XR_YR_Z(0\ 0\ l_U)^T + (*)_U,\ ((*)=\mathrm{a, b, c, d}) \quad \text{(A-14)}$$

The torque working at the universal joint is obtained by

$$\tau_U = \textstyle\sum_{i=\mathrm{a,b,c,d}}(F_i \times r_i) \quad \text{(A-15)}$$

where, "x" means outer product. Since τ_U is a linear equation with respect to $\Delta\theta_x$, $\Delta\theta_Y$, $\Delta\theta_Z$ it can be rewritten as,

$$\Delta\tau_U = \left[\frac{\partial\tau_U}{\partial\Delta\theta_x}\ \frac{\partial\tau_U}{\partial\Delta\theta_Y}\ \frac{\partial\tau_U}{\partial\Delta\theta_Z}\right](\Delta\theta_X\ \Delta\theta_Y\ \Delta\theta_Z)^T \quad \text{(A-16)}$$

With S_U representing a stiffness matrix at the universal joint, τ_U is obtained by,

$$\Delta\tau_U = S_UR_XR_YR_Z(\Delta\theta_X\ \Delta\theta_Y\ \Delta\theta_Z)^T \quad \text{(A-17)}$$

Equating (A-16) and (A-17), the stiffness matrix is obtained by,

$$S_U = \left[\frac{\partial\tau_U}{\partial\Delta\theta_x}\ \frac{\partial\tau_U}{\partial\Delta\theta_Y}\ \frac{\partial\tau_U}{\partial\Delta\theta_Z}\right](R_XR_YR_Z)^T \quad \text{(A-18)}$$